Metallophysics and Advanced Technologies
Металофіз. новітні технол.
Metallofiz. Noveishie Tekhnol.
2023, vol. 45, No. 11, pp. 1349–1384
https://doi.org/10.15407/mfint.45.11.1349
Reprints available directly from the publisher

PACS numbers: 42.60.Jf, 47.40.Rs, 62.50.Ef, 81.20.Ka, 82.33.Vx, 82.40.Fp, 89.20.Bb

Profiled Detonation Waves in the Technologies of Explosion Treatment of Metals

V. V. Sobolev, O. V. Skobenko, M. M. Kononenko, V. V. Kulivar, and A. V. Kurlyak*

Dnipro University of Technology,
19 Academician Dmytro Yavornytsky Ave.,
UA-49005 Dnipro, Ukraine
**State Enterprise "Scientific and Production Association 'Pavlohrad Chemical Plant'",*
44 Zavodska Str.,
UA-51402 Pavlohrad, Ukraine

A short review is represented concerning physicotechnical features of current technologies, plane-wave, converging cylindrical and spherical detonation waves used in physics and chemistry of high energy densities, physics of metals, materials science, machine building, and mining and metallurgical industry. The main drawbacks of existing technologies are shown, and attention is focused on the technical nature of the reasons limiting their application. Attention is paid to solving the problem of simultaneous initiation of detonation of the entire surface layer of a light-sensitive explosive, regardless of the shape of the surface. A physical and mathematical methodology for estimating shock-wave parameters of an explosive during initiation of detonation in it by explosion of the initiation layer of the charge of a light-sensitive explosive composite is proposed. Prospects of practical application of detonation (shock) waves of the specified profile formed by laser ignition of the surface of a light-sensitive explosive composite are discussed. Physicochemical potential of the system of laser initiation of detonation makes it possible to form any wave profiles and get pulses of the intensity from 0.1 to 1.0 kPa·s on the surfaces being more than 1 m^2. Precision and safe system of laser initiation can be used during any types of blasting operations including the ones that cannot be implemented principally, while applying standard systems for initiating explosives and means of explosion.

Corresponding author: Valery Viktorovych Sobolev
E-mail: velo1947@ukr.net

Citation: V. V. Sobolev, O. V. Skobenko, M. M. Kononenko, V. V. Kulivar, and A. V. Kurlyak, Profiled Detonation Waves in the Technologies of Explosion Treatment of Metals, *Metallofiz. Noveishie Tekhnol.*, **45**, No. 11: 1349–1384 (2019).
DOI: 10.15407/mfint.45.11.1349

Key words: light-sensitive explosion composite, laser, radiation, chemical reactions, detonation, wave fronts, shockwaves, super-short pulse.

Подано короткий огляд фізико-технічних особливостей сучасних технологій пласкохвильової, збіжної циліндричної та сферичної детонаційних хвиль, що використовуються у фізиці та хемії високих густин енергії, фізиці металів, матеріялознавстві, машинобудуванні, гірничо-металурґійній промисловості. Показано основні недоліки наявних технологій і зосереджено увагу на технічному характері причин, що обмежують застосування їх. Приділено увагу вирішенню проблеми одночасного ініціювання детонації всього поверхневого шару світлочутливої вибухової речовини, незалежно від форми поверхні. Запропоновано фізико-математичну методику оцінки ударно-хвильових параметрів вибухової речовини під час ініціювання в ній детонації вибухом ініціяційного шару заряду світлочутливого вибухового композиту. Обговорено перспективи практичного застосування детонаційних (ударних) хвиль заданого профілю, що утворюються під час лазерного запалення поверхні світлочутливого вибухового композиту. Фізико-хемічний потенціял системи лазерного ініціювання детонації уможливлює формувати будь-які профілі хвиль і одержувати імпульси інтенсивністю від 0,1 до 1,0 кПа·с на поверхнях більше 1 м^2. Прецизійна та безпечна система лазерного ініціювання може бути використана під час будь-яких видів вибухових робіт, у тому числі тих, які принципово не можуть бути реалізовані за застосування стандартних систем ініціювання вибухових речовин і засобів вибуху.

Ключові слова: світлочутливий вибуховий композит, лазер, випромінювання, хемічні реакції, детонація, хвильові фронти, ударні хвилі, надкороткий імпульс.

(Received 8 June, 2023; in final version, 15 July, 2023)

1. INTRODUCTION

Studies of the regularities of changes in physicochemical properties of substances and phenomena occurring in the materials under shock-wave action are aimed at solving scientific problems of mostly fundamental nature along with creating new technologies and materials. Currently, being independent scientific and technical areas, shock wave technologies are uncontested and cost-effective, having no competitors in many respects. The most well-known technologies are various methods for the production of detonation nanosize diamond crystals [1–3], synthetic diamond micropowders [4–6], monocrystals [7, 8], superhard modifications of boron nitride [9, 10], cubic silicon nitride [11], chaoite [12, 13] and its transformations [14] into carbon phases as well as other superhard materials. The technologies of explosion stamping [15], hardening and explosion welding [16, 17], powder compaction [18], *etc.* are being developed successfully. Shock action is applied to change shape and density of materials, their conductivity, strength, crystal-

line structure, defectiveness, chemical activity, refractive index, valence of chemical elements and even isotopic composition, absorption spectra, and other physical and chemical properties of substances.

A significant contribution to the development of shock-wave studies was made by the research carried out especially intensively during the Second World War and the following years after its completion. According to the programme of works in the frameworks of the USSR nuclear project, there were investigations concerning the method of initiating a chain reaction using chemical explosives along with the planned studies of the shock-wave parameters of minerals, rocks, metals, and other materials at high temperatures and pressures [19–21]. Scientists and engineers from Germany, the USA, the USSR, and Great Britain were the first researchers and world leaders. In the early 1960s, reports on the results of scientific studies of the shock wave effect on substances began to appear regularly in open sources of information in Poland, France, Japan, and some other countries. During the recent three decades, the list of countries has expanded significantly; each of the country has a growing number of research and production organizations specializing in the development and application of explosive technologies.

In the process of shock wave processing of materials, regular industrial explosives (ammonites, octogen, hexogen, heating elements, plastic explosives, *etc.*) and various methods of priming are used. The selection of methods depends on the operating conditions, safety requirements, technical and economic feasibility. A method of non-electric priming using a detonating cap (DC) and an electrical priming system, which main element is an electric detonator (ED), are the most widely used techniques. From the viewpoint of any of the selected explosive treatment technologies using ED, DC, and any priming system, the explosive is a point source of excitation. In this regard, all known material processing schemes were developed taking into account technological capabilities of ED and a blasting method. When detonation is initiated in explosive charges by an electric detonator explosion, a front of a diverging detonation wave propagates from the point of initiation. It is obvious that the sliding front of a detonation wave (and of a shock wave, respectively) limits the possibility of expanding a range of products with complex relief and large surface area. Problems arise especially when a very short pulse action (up to 1 μs) is required in terms of simultaneous excitation of detonation over the whole explosive surface.

2. METHODS AND FOCUS AREAS OF THE SHOCK-WAVE COMPRESSION TECHNOLOGY

In the context of experimental studies and technological processes, materials are processed using following main varieties of shock-wave

profiles: 1—by a linear wave front sliding at an angle of inclination α to the material surface ($0° < \alpha \leq 90°$); 2—by a plane-wave front, impact angle with the material surface as well as impact angle of the shock wave fronts or detonation waves is at 0°; 3—by an axisymmetric (cylindrical) wave front converging to the axis of symmetry; 4—by a symmetrical front with respect to a point (spherical),as a rule, the action of a spherical converging front on the material is studied; 5—by a Mach wave front (the result of irregular impact of oblique waves to the axis of symmetry or collision of two plane fronts of detonation or shock waves); and 6—self-organization of the detonation wave profile in the explosive charge initiated by the explosion of an electric detonator or a detonating cap.

Most methods indicate the formation of detonation waves of a specified profile using two different explosives: an initiating high-velocity explosive with a detonation velocity $D1$ and the main explosive charge with a detonation velocity $D2$ ($D1 > D2$) [22–24] using systems (or methods) of electric or non-electric initiation.

Some of the most common schemes of shock wave processing of materials are shown in Fig. 1. a linear front of a detonation wave sliding over a flat surface can be created in several ways, one of which is represented in Fig. 1, *a* (*1*—detonator; *2*—direction of the detonation wave front motion; *3*—linear-wave generator of the explosive charge; *4*—origination of the detonation front in the main explosive charge *5*; *6*—front of the plane detonation wave and its direction *7*). One type of explosive is used in a device of that kind.

A scheme of a plane-wave generator is demonstrated in Fig. 1, *b* (*1*—detonator; *2* and *3*—plane-wave generator consisting of charges of explosive *1* with $D1$ and explosive *2* with $D2 < D1$, respectively; *3*, *a*—main explosive charge; *4*—thrown striker plate; *5*—test sample; *6*—metal matrix to preserve the sample after its shock compression). This figure shows the most well-known scheme of an explosive plane wave front generator used in the SHM synthesis technology, studies of the matter properties at high pressures, and solution of many other problems in shock wave physics.

A converging cylindrical front of a detonation or shock wave is obtained using generators of various designs. One of their diagrams is shown in Fig. 1, *c*. Shock waves converging to the axis are used mainly in experimental physics, *i.e.*, for creating high-power lasers, studying cumulative flows, analysing fundamental possibility of obtaining thermonuclear temperatures, *etc*. Following designations are taken for the diagram in Fig. 1, *c*: *1*—generator of a converging circular front of a detonation wave; *2*—main explosive charge; *3*—cylindrical workpiece; *4*—detonator; *5*—arrows indicating direction of the detonation front motion; *6*—lens made from an inert substance. Devices with axisymmetric arrangement of elements (cylindrical ampoules) (Fig. 1, *d*),

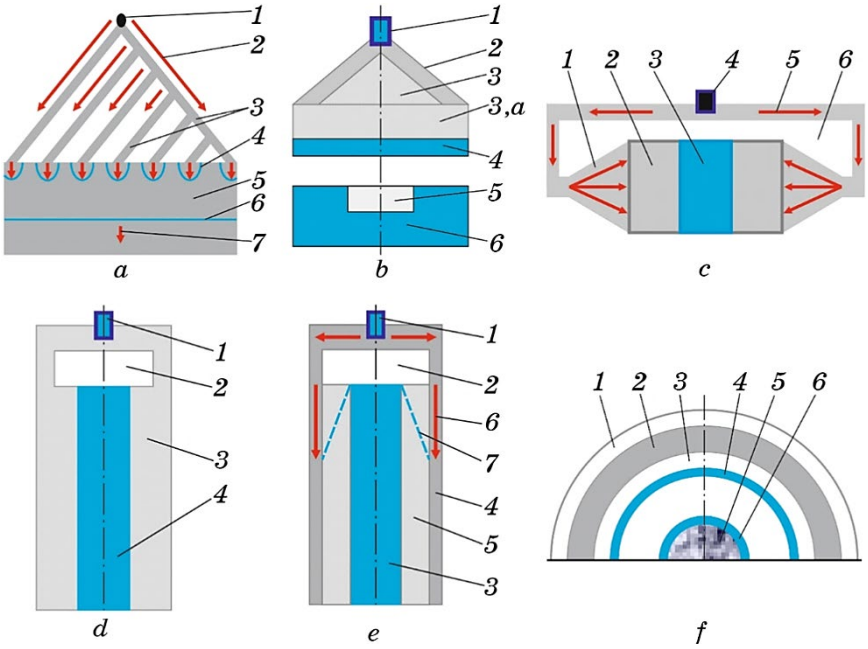

Fig. 1. Simplified diagrams of some generators of profiled detonation waves: linear-wave (*a*), plane-wave (*b*), cylindrical front of a converging detonation wave (*c*), sliding wave front along the generatrix of a cylinder at an angle of 90° (*d*), sliding wave front along the generatrix of a cylinder at a given angle being less than 90° (*e*), scheme of an explosive generator with throwing of a hemispherical shell (*f*).

are used in the technology of synthesis of dense modifications of boron nitride, diamond, chaoite, many chemical compounds, crushing of superhard materials, welding and hardening of metals. It is also used in studies of regularities of changes in the properties of shock-treated substances, hydrodynamic flows of matter behind the shock front, *i.e.*, analysis of specific features in the development of vortices and turbulent supersonic flows is an urgent task of modern gas dynamics and physics of high energy concentrations. Such problems arise when studying the entry of space objects into the dense layers of the Earth's atmosphere, *etc*. It is possible to change a shock wave profile in the processed material in cylindrical ampoules by changing the geometric ratios of structural elements and characteristics of explosive charges.

Thus, incident shock waves in a porous material can have following profiles: they do not reach the axis (weak); meet near the axis (medium); collide near the axis, representing a cone in space (strong); and are very strong when the Mach (head) wave front is formed near the axis. In the first three examples, the material is processed relatively

evenly across the cross section. In the latter case, the wave front is called a three-wave shock configuration, representing a truncated cone in space, which smaller base is called the Mach front. The pressure and temperature in the Mach wave front are several times higher than the pressure and temperature of the incident shock waves. The main elements of the device are as follows: *1*—detonator; *2*—lens; *3*—explosive charge; *4*—workpiece of a cylindrical shape (a striker pipe, inside which there is a container with the material under study and other variants of elements).

A similar cylindrical device is demonstrated in the diagram in Fig. 1, *e*. The main designations of structural elements are as follows: *1*—detonator; *2*—lens; *3*—cylindrical workpiece; *4*—layer of high-velocity (active) charge with a detonation velocity $D1$; *5*—main explosive charge (passive) with a detonation velocity $D2$ ($D2 < D1$); *6*—arrow indicating direction of the detonation front motion in the active explosive; *7*—incident front of a detonation wave in the passive explosive charge. Unlike the design in Fig. 1, *d*, the front inclination in a device with a generator of a given detonation wave profile Fig. 1, *e* can vary depending on the $D2/D1$ ratio.

First, the issue of technical implementation of the spherical cumulation of detonation waves (implosive explosion) was studied in secrecy during the development of the first samples of nuclear weapons. The idea was implemented by blasting the explosive charge in the form of a ball with electric detonators installed on its surface, equidistant from each other. Creation of a spherical converging profile of a detonation wave is not a simple process, requiring long-term preparation. To develop extremely high pressures in the materials under study, a method for exploding hemispheres was proposed. Figure 1, *f* shows a diagram of an explosive generator with the explosion products that throw a metal hemispherical shell [25]. The figure numbers indicate following elements of the device: *1*—generator of a spherical converging detonation wave; *2*—hemispherical propellant explosive charge; *3*—air gap; *4*—hemispherical steel shell (striker); *5*—test material; *6*—hemispherical metal shell.

The experience of the authors of the above-cited works indicates that creation of detonation waves (shock waves) with the specified front profile does not require necessarily the use of a special device with charges of two explosive types. Sometimes, when using explosive charges weighing up to 1 kg, it is possible to apply multipoint initiation or a blasting method using metal foils or wires (a current pulse with a duration of 10^{-5}–10^{-7} s and a density of 10^4–10^6 A·mm^{-2}) as well as other designs, which description can be found in [20, 22–26].

Practical implementation of any design of an explosive generator requires additional mass of explosives to the main charge, which sometimes amounts to at least half the mass of the main charge. However,

use of such generators is expedient for blasting small explosive charges, limited to two or three dozen kilograms, applied in experimental physical studies or under industrial conditions in the SHM synthesis or pressure treatment of small-size metal structures. Pressure treatment of complex-relief surfaces often results in insurmountable technical difficulties associated with the shortcomings of modern means of initiation and properties of explosives. For example, to create a plane wave using the scheme in Fig. 1, *b*, a plane wave generator will require 1.3–1.7 times more explosive than for the main charge. When using small masses of explosives, the problem is solved without any difficulties. However, with an increasing area of the treated surface, the task becomes rather demanding and inexpedient both technically and economically.

The disadvantage of using blasting tools (detonating cap, electric detonator, igniter cord, waveguide of a non-electric initiation system, *etc.*) is that detonation in the explosive charge starts at the points of contact of the corresponding means of initiation. Simultaneous excitation of a detonation wave (hence, a shock wave in a material) over large areas and complex-shape surfaces is currently either not feasible or, at best, is associated with great practical difficulties.

Testing the strength of samples of multifunctional coatings of aircraft bodies (missiles) and stability of structures, where it is necessary to create low-power pulses with the duration of less than 1 μs, is one of the features of simulation modelling of the effects of pulse radiation of x-ray combat lasers [27, 28]. The problem here is that it is impossible to achieve short pulses when testing real structures with the area of more than 1 m^2 by any method of shock-wave action using standard explosives and initiation devices. It is possible to expend a large amount of light pulse energy to excite detonation simultaneously on a large area surface; however, there have been no reports of the results of such experiments so far.

An issue of standardization of experimental studies using explosives, methods, and means of priming remains topical. A problem of standardization and methodological support of the experimental works as well as testing of light-sensitive compounds and blasting means is one of the urgent problems of experimental physics of explosion.

3. EXPERIMENTAL AND THEORETICAL STUDIES

A system of laser initiation of explosives is selected as the basis for the proposed method of shock-wave processing of materials by profiled waves. The method specifics is in simultaneous ignition of the entire surface of the light-sensitive explosive composite (LSEC) by an expanded beam of laser pulse radiation. LSEC is ignited over the entire surface exposed to radiation. LSEC is applied to the surface of the explosive

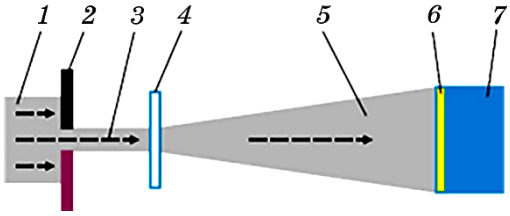

Fig. 2. Scheme of initiating a light-sensitive explosive composite by laser radiation: laser beam (*1*), diaphragm (*2*), laser beam after diaphragm (*3*), diverging lens (*4*), scattered laser beam (*5*), LSEC layer (*6*), explosive charge or the processed material (*7*).

charge *7* (Fig. 2) or immediately on the surface of the processed material *7*. The surface, on which the light-sensitive layer of the explosive composite is applied, and except for the plane, may have other profiles.

As it is seen from a simple diagram, a laser beam passes through a diaphragm that transmits the central part of the beam, which is characterized by maximum energy. After that, the beam is expanded by a diverging lens and irradiates the surface of the light-sensitive composite. This method of initiation is convenient since detonation is excited simultaneously on the entire surface exposed to laser radiation. Solid-state lasers on neodymium-activated glass were used as a radiation source (Table 1). Wavelength of radiation is $\lambda = 1.06$ μm; pulse duration at half-maximum is $\tau_q = 11$ ns.

When studying LSEC sensitivity, various types of polymers were used, and their concentration varied too. As a result, composites were obtained, which critical initiation energy densities were within the range of 2.3–40.0 mJ/cm^2 [29–31]. According to [30, 32], the sensitivity level of such energy-saturated explosive compounds as EC2, EC7, EC16, EC17, and LSEC-1 (*Ukr.* BC2 (VS2), BC7, BC16, BC17, and СВК-1 (SVK-1)) (Table 2) is 1–2 orders of magnitude higher than the sensitivity of standard primary explosives, *e.g.*, lead azide, lead trinitroresorcinate, and fulminate of mercury. It should be noted that it would be impossible to conduct research without synthesized explosive com-

TABLE 1. Operating characteristics of lasers.

Characteristics	Laser number			
	1	2	3	4
Threshold voltage $U_{\text{threshold}}$, V	1400	1450	1400	1400
Threshold pump energy $E_{\text{threshold}}$, J	98	105	101	98
Output energy of pulse generation E_{kp}, J	0.18	0.17	0.18	0.19

TABLE 2. Explosive characteristics of some light-sensitive composites [29, 30, 34, 35].

LSEC	Density ρ, kg/m^3	Detonation velocity D, m/s	Critical density of ignition energy E, J/cm^2	Critical energy E, J
EC2	3000	6500	2.3×10^{-3}	1.1×10^{-5}
EC7	4600	–	5×10^{-3}	50.3×10^{-5}
EC16	1100	5100	12×10^{-3}	57.5×10^{-5}
EC17	1800	6700	40×10^{-3}	136×10^{-5}
LSEC-1	2100	4850	24×10^{-3}	76×10^{-5}

posites, being anomalously sensitive to laser radiation.

Pulse laser initiation of regular explosives with different sensitivities was studied in a number of theoretical and experimental works by A. A. Brish, I. A. Galeev, and V. N. Zaitsev, 1966; E. I. Aleksandrov and A. G. Vozniuk, 1978; Yu. F. Karabanov and V. K. Bobolev, 1981; V. N. Viliunov, 1984, and others. While analysing the results obtained in the listed works, it was found that there is no unified measurement technique. This circumstance was the basis for the development of a new technique for measuring the pulse of explosion products and sensitivity of explosives to laser initiation. Compared with the known studies, the new technique has made it possible to improve significantly the measurement accuracy [33].

Following LSECs were used in the experiments: EC2, LSEC-1 based on lead azide, and EC17. The attractiveness of using the EC2 composite is in its extremely high sensitivity to laser pulse radiation—its initiation threshold is lower than that of pressed lead azide [29, 32]. We used EC2 in a limited amount (for the samples with a surface of no more than 100 cm^2), mainly because of the relatively complex synthesis technology. Production of the LSEC-1 composite was technologically convenient, since the chemical plant, where the experimental work was carried out, produced lead azide. However, the content of lead azide in LSEC-1 is the main disadvantage of this composite. Use of composite EC17 on an area of up to 0.5 m^2 is stipulated by the fact that it satisfies almost all requirements of technical and environmental safety; moreover, it is characterized by the available initial components and a relatively simple production technology. EC17 is based on such explosive substance as urotropine peroxide. Its characteristics are as follows [36, 37]: oxygen balance is of –92.2%; explosion heat is of 5080 kJ/kg; explosion temperature is of 2370°C; and gas volume is of 813 l/kg. It detonates from the impact, from the flame of an igniter cord. The minimum charge for tetryl is of 0.05 g; the TNT equivalent is 1.

To obtain a light-sensitive explosive composite and apply it as a coating on an explosive charge or on a material being processed, the technology of preparing a viscous base, being a suspension of explosive powder in a polymer solution, was used [38]. Explosive composites of the EC, LSEC-1 grades and new blasting tools based on them make it possible to expand considerably a range of types of blasting operations and areas of application of explosion energy. Light-sensitive explosive composites of abnormally high sensitivity to pulsed laser action form a new class of primary initiating explosives. Depending on the tasks set and the conditions for carrying out blasting, detonation in explosive charges can be excited either by transmitting a laser pulse through a light-fibre cable or through an air atmosphere by direct action of a narrow or expanded radiation beam on the surface of a light-sensitive composite (Fig. 2).

A method of forming profiled detonation waves using LSEC charges was tested taking into account dependences of the energy and density of ignition energy on the binder component concentration [29, 30] as well as dependence of the irradiation spot diameter [39] and ignition delay time on the radiation energy density [31, 40, 41]. It was established [40] that lead azide sensitivity in a composite (phlegmatized lead azide) to mechanical impacts is at the level of secondary initiating explosives. The results of studies obtained during LSEC initiation by plane detonation waves were also taken into account [42–44].

The explosives were manufactured and experimental studies were carried out at the State Enterprise "Scientific and Production Association 'Pavlohrad Chemical Plant'". Trial explosions of small-mass single explosive charges were performed both in the explosive section and in a special experimental drift.

3.1. Estimation of Shock-Wave Parameters in the Explosive Charge When Initiated by a Plane Detonation Front

Detonation in the explosive charge (passive explosive charge, PE) is excited by the plane front of a detonation wave of the active explosive charge (AE), which role is played by the LSEC layer (Fig. 2). Detonation characteristics and dynamic compressibility for PE (hexogen charge) are taken from [22]. The calculations were carried out taking into account following assumptions about the state behind the front of a refracted wave: 1—refracted wave–shock wave. There is no chemical reaction behind the wave front. The shock compressibility of PE is linear and is described by linear equation $D = a + bu$ (where D, u are wave and mass velocities, respectively; a is speed of sound; b is constant); 2—refracted wave—detonation wave. Behind its front, a state of detonation products (DP) is described by a polytropic equation of maximum heat release; 3—refraction of the detonation wave from the AE and PE

occurs according to the shock wave mechanism; 4—shock adiabat and isentrope of AE detonation products coincide. The initial densities of AE (ρ_{01},) and PE (ρ_{02}) are related by the ratio $\rho_{01} > \rho_{02}$.

The front of a plane detonation wave in the AE layer propagates to the interface, whose initial parameters are described by the equations [45]

$$U_{H1} = D_{H1}\left(K_1 + 1\right)^{-1},\ C_{H1} = D_{H1}\left(K_1 + 1\right)^{-1}, \tag{1}$$

$$\rho_{H1} = \rho_{01}\left(K_1 + 1\right)\left(K_1\right)^{-1},\ P_{H1} = \rho_{01}\left(D_{H1}\right)^2\left(K_1 + 1\right)^{-1}, \tag{1}$$

where U_{H1} is mass velocity of particles behind the detonation front; C_{H1} is speed of sound; D_{H1} is detonation velocity; ρ_{H1} is density; P_{H1} is pressure; K is adiabatic index of the detonation products at the Chapman–Jouguet point for the AE layer.

When a detonation wave passes the interface, reflection occurs, as a result of which either a shock wave or a rarefaction wave appears in DP; in the second explosive (PE), there is a shock wave. Obviously, if DP shock compressibility of the AE layer is less than DP shock compressibility of the PE layer, a rarefaction wave will go through the explosion products of AE and following condition will be satisfied at the interface between the layers with different densities

$$U_{x1} = U_{H1}m + \Delta U_1, \tag{2}$$

where U_{x1} is speed of the surface motion; ΔU_1 is velocity increment of the detonation products in the rarefaction wave propagating along DP of the AE layer. Increment ΔU_1 is determined by the Riemann integral [45]:

$$\Delta U_1 = \int_{P_{x1}}^{P_{H1}} \frac{dP}{C_1\rho_1} = \int_{U_{H1}}^{U_{x1}} \sqrt{-dPdU_1}. \tag{3}$$

The integration limits are taken from the final pressure P_{x1} to the initial pressure P_{H1}. The integrand includes density ρ_1 and speed of sound C_1 in DP of the AE layer. For DP of the AE layer, we will consider the isentropic law that relates pressure and density in the expanding detonation products to be valid, *i.e.*,

$$P_1 = A_1\rho_1^{K_1}, \tag{4}$$

where A_1 is AE constant; $A_1 = P\upsilon = P/\rho$, $\upsilon_{H1} = 1/\rho_{H1}$ are specific volume of PD. Then,

$$C_1^2 = \frac{dP}{d\rho}A_1K_1\rho_1^{K_1-1},$$

$$\frac{C_1}{C_{H1}} = \left(\frac{\rho_1}{\rho_{H1}}\right)^{K_1-1} = \left(\frac{P_{x1}}{P_{H1}}\right)^{\frac{K_1-1}{2K_1}}, \tag{5}$$

$$\frac{\rho_1}{\rho_{H1}} = \left(\frac{P_{x1}}{P_{H1}}\right)^{\frac{1}{K_1}}.$$

Having substituted the literal values for ρ_1 and C_1 from (5) into equation (3), after simple transformations, we obtain

$$\Delta U_1 = \frac{2K_1 P_{H1}}{(K_1-1)\rho_{H1} C_{H1}}\left[1 - \left(\frac{P_{x1}}{P_{H1}}\right)^{\frac{K_1-1}{2K_1}}\right]. \tag{6}$$

However, since $C^2 = K_1 P_{H1}/\rho_{H1}$ and $C_{H1} = D_{H1}K_1/(K_1+1)$,

$$\Delta U_1 = \frac{2K_1 D_{H1}}{K_1^2-1}\left[1 - \left(\frac{P_{x1}}{P_{H1}}\right)^{\frac{K_1-1}{K_1}}\right]. \tag{7}$$

Then, condition (2) will be as follows:

$$U_{x1} = U_{H1} + \frac{2K_1 D_{H1}}{K_1^2-1}\left[1 - \left(\frac{P_{x1}}{P_{H1}}\right)^{\frac{K_1-1}{2K_1}}\right]. \tag{8}$$

Taking into consideration (1), we can express

$$U_{x1} = \frac{D_{H1}}{K_1+1}\left\{1 + \frac{2K_1}{K_1-1}\left[1 - \left(\frac{P_{x1}}{P_{H1}}\right)^{\frac{K_1-1}{2K_1}}\right]\right\}; \tag{9}$$

from here,

$$P_{x1} = P_{H1}\left[\frac{3K_1-1}{2K_1} - \frac{K_1^2-1}{2K_1}\cdot\frac{U_{x1}}{D_{H1}}\right]^{\frac{2K_1}{K_1-1}}. \tag{10}$$

By relating the pressure in a rarefaction wave to the magnitude of a mass velocity, we will have

$$P_{x1} = P_{H1}\left[\frac{3K_1-1}{2K_1} - \frac{K_1^2-1}{2K_1}\cdot\frac{U_{x1}}{U_{H1}}\right]^{\frac{2K_1}{K_1-1}}. \tag{11}$$

At the moment of exit of the initiating detonation wave, a mode is established at the interface between two explosive layers. In terms of this mode, pressure P_{x2} and corresponding mass velocity U_{x2} of particles in the layer of explosives behind the front of the excited shock or detonation wave will be equal to the pressure and mass velocity of the expanding detonation products of the PE layer, *i.e.*,

$$P_{z1} = P_{x2}, \quad U_{x1} = U_{x2}. \tag{12}$$

Consider the case when a refracted wave is a shock wave, there is no chemical reaction behind its front, and a state of the shock-compressed medium is approximated by the equation

$$D = a + bu. \tag{13}$$

Shock adiabats of many explosives can be constructed basing on the techniques described in [46]. Thus, shock compressibility of explosives (TNT, RDX, nitroglycerin, *etc.*) is of following form [47]

$$D = C_0 + 2U - 0.1U^2 / C_0, \tag{14}$$

and for salts of various acids,

$$D = C_0 + 1.5U - 0.05U^2 / C_0. \tag{15}$$

Based on Eq. (13), the relation between pressure and density for explosives is approximated using following equation

$$P = \frac{\rho_0 a^2 \left(1 - \rho_0 / \rho\right)}{\left[1 - B\left(1 - \rho_0 / \rho\right)\right]^2}, \tag{16}$$

equations in Theta form

$$P = A\left[\left(\rho/\rho_0\right)^n - 1\right], \tag{17}$$

or equations

$$P = B\left(\rho/\sigma_0\right)^m + c, \tag{18}$$

where A, B, n, m, C are compressibility parameters of the PE. The procedure for transition from equation (16) to equations (17) and (18) is described in detail in [48].

Taking into account the laws of conservation of mass, pulse, and energy described by the gas dynamics equations [49] and one of the shock adiabatic equations (16)–(18), we obtain the dependence of pressure on

the velocity of medium flow behind the shock wave front. For the shock adiabat of form (16), the dependence will be as follows:

$$U_{x2} = \frac{\sqrt{\left(4bP_{x2}U_{02}\right)^2 + a^2} - a}{2b}; \tag{19}$$

for the shock adiabats of forms (17) and (18), respectively, we obtain

$$U_{x2} = \sqrt{P_{x2}U_{02}\left[1 - \left(1 + P_{x2} / A\right)^{\frac{1}{n}}\right]}, \tag{20}$$

$$U_{x2} = \sqrt{P_{x2}U_{02}\left[1 - \left(\frac{P_{x2} - C}{B}\right)^{\frac{1}{n}}\right]}. \tag{21}$$

Thus, for the case when a plane detonation wave of the initiating AE excites a shock wave in PE, the parameters of the latter are determined by joint solution of one of the equations (19)–(21) and equation (9) using condition (12) on the contact interface between the AE and PE layers. Equating U_{x1} of mass velocity from (9), *i.e.*, $U_{x1} = U_{x2}$, depending on the accepted form of the shock adiabatic equation, we will have

$$U_{x1} = \frac{D_{H1}}{K_1 + 1}\left\{1 + \frac{2K_1}{K_1 - 1}\left[1 - \left(\frac{P_{x1}}{P_{H1}}\right)^{\frac{K_1 - 1}{2K_1}}\right]\right\} = \tag{22}$$

$$= U_{x2} = \frac{\sqrt{\left(4bP_{x2}U_{02}\right)^2 + a^2} - a}{2b},$$

$$U_{x1} = \frac{D_{H1}}{K_1 + 1}\left\{1 + \frac{2K_1}{K_1 - 1}\left[1 - \left(\frac{P_{x1}}{P_{H1}}\right)^{\frac{K_1 - 1}{2K_1}}\right]\right\} = \tag{23}$$

$$= U_{x2} = \sqrt{P_{x2}U_{02}\left[1 - \left(1 + P_{x2} / A\right)^{\frac{1}{n}}\right]},$$

$$U_{x1} = \frac{D_{H1}}{K_1 + 1}\left\{1 + \frac{2K_1}{K_1 - 1}\left[1 - \left(\frac{P_{x1}}{P_{H1}}\right)^{\frac{K_1 - 1}{2K_1}}\right]\right\} = \tag{24}$$

$$= U_{x2} = \sqrt{P_{x2}U_{02}\left[1 - \left(\frac{P_{x2} - C}{B}\right)^{\frac{1}{n}}\right]}.$$

Obviously, solution of any of Eqs. (22)–(24) will be such a value of P_x, P_{x1}, P_{x2}, when the right and left parts of these equations will be equal. This problem is most simply solved graphically by plotting in the P-u coordinates an isentrope of DP expansion of the AE layer from the Chapman–Jouguet state and a shock adiabat of the analysed explosive.

When organizing a numerical solution with the preset degree of accuracy, it is convenient to use an iteration method, taking the value $P_{x1} = P_{H1}$ as a zero approximation.

The performed studies have shown that transition of a detonation wave from AE to PE is accompanied by the formation of an overcompressed detonation in the latter, provided that the characteristic dimensions of the PE charge exceed the critical ones. An 'undercompressed' detonation wave is possible in case when the transition is carried out from a less powerful AE to a more powerful PE; in this context, a detonation mode in the calculations was estimated not from the ideal detonation velocities of two explosives but from the pressures in the incident and refracted waves. The issue of mutual influence of the finite dimensions of the charges of two explosives on the occurrence and propagation of incident and refracted detonation waves was not considered in this study.

The proposed method for estimating and predicting the initial parameters of the 'imposed' detonation is used in gas-dynamic calculations when selecting the types of explosives in the designs of plane-wave generators and bilayer explosive charges.

3.2. Results of the Measurement of LSEC Flash Delay

When determining the explosion delay time from the beginning of the laser pulse action, the dependence of time on the polymer binder content (Fig. 3) and radiation energy was determined experimentally (Fig. 4). Figure 3 represents the dependences of ignition time delay of the samples of photosensitive explosive composites on the density of laser energy at mass polymer concentration (%).

It has been defined experimentally [29] that EC2 samples containing 15% of polymer demonstrate a longer ignition time delay than the ones containing 20%. At first glance, everything should be *vice versa*. First, the area of laser energy release in EC2 samples, containing 15% of polymer, is smaller than in EC2 with 20%; thus, heating of the subsurface layer of the substance in such explosive composites should be carried out more efficiently. Secondly, the higher the explosive content in LSEC is, the shorter the flash delay time should be.

However, according to the results of studies [30], the regularity is fundamentally different. In our opinion, the emphasized fact indicates that the induction time of LSEC ignition is determined by the time of the ignition source formation, and the time of transition from combus-

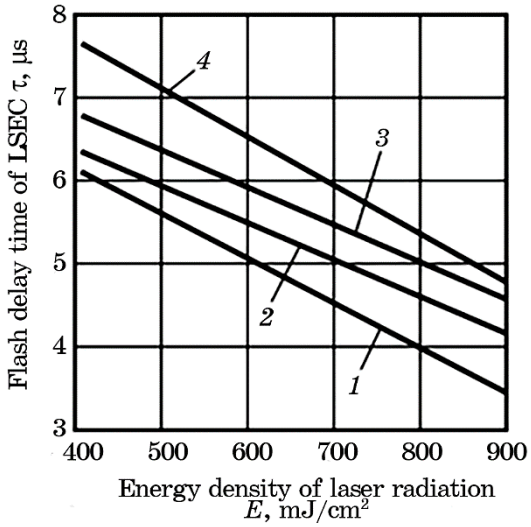

Fig. 3. Dependence of the delay time of LSEC initiation on the energy of laser radiation density: EC2 (30%) (*1*), EC1 (15%) (*2*), LSEC-1 (30%) (*3*), LSEC-1 (20%) (*4*).

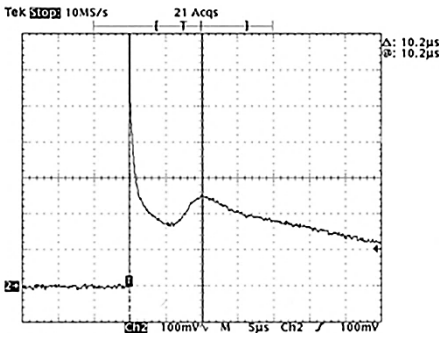

Fig. 4. Oscillogram of the records of LSEC delay time relative to laser pulse (in terms of EC17).

tion to detonation is a small part of the total recorded ignition delay time. Therefore, laser detonation of LSEC is determined primarily by deformation unloading of the substance in the ignition source.

Figure 4 shows that the first peak corresponds to the laser pulse, and the second one corresponds to the maximum of light radiation emanating from the explosion products. When LSEC detonation is initiated by wide beams ($d = 3$–4 mm) with a critical laser energy density, no changes are observed on the surface of LSEC sample. When initiated by narrow laser beams ($d < 1$ mm), in case of failure, slight colour changes of

LSEC occurred; however, no failure of the composite was observed. We consider that the nature of the changes indicates that the laser ignition process occurs at a low average surface temperature of LSEC.

To confirm this conclusion, spectrophotometric measurements of the reflection coefficient and absorption index of LSEC were carried out. The methods and recommendations given in [38] were applied. From practical, economic, and environmental-safety considerations, LSEC of EC17 grade (20% of binder) was selected. To measure optical properties, the EC17 sample was exposed to radiation from a low-power laser with a radiation wavelength of 1.06 μm. The angle of radiation incidence did not exceed 5° relative to the normal. It has been found that the diffuse reflection coefficient of LSEC samples is ≅ 80%. The intensity peaks of the reflected light in front of LSEC sample correspond to the reflection from the lacquer that was used when coating LSEC on glass. A large value of the diffuse reflection coefficient is not unique; most likely it confirms the fact that explosives have high reflectivity at the laser wavelength, $\lambda = 1.06$ μm. The absorption index is at the level of about 100 cm^{-1}. Unfortunately, the exact value of the index could not be determined due to practical difficulties in fabricating thin and translucent LSEC samples.

The nature of energy density distribution in the laser beam in the horizontal and vertical profiles corresponds to the normal distribution law (Fig. 5).

In terms of EC2 with a binder concentration of 20% (as a composite with anomalous sensitivity to laser radiation), having heat capacity $C_p \cong 0.4$ J/g·K, density $\rho = 4.0$ g/cm^3 at the critical impact energy densi-

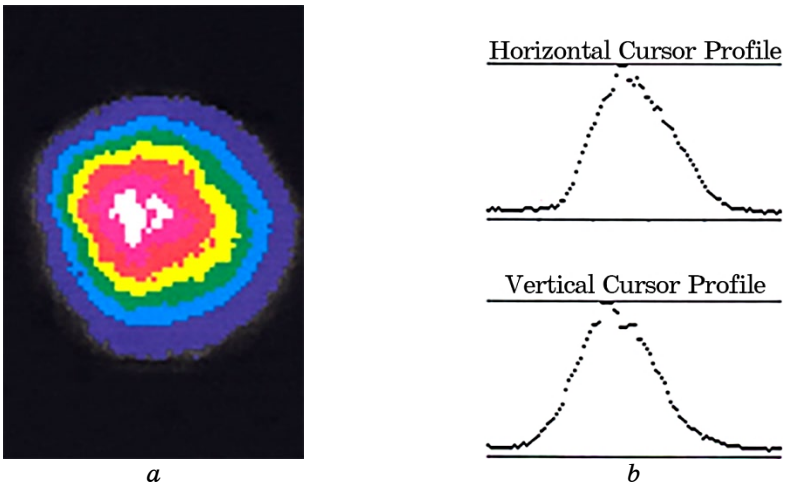

Fig. 5. Distribution of energy density in a laser beam: in a print (*a*), horizontal and vertical profile (*b*).

ty $E_{kp} \cong 0.5$ J/cm^2, the heating temperature is approximately equal to:

$$\Delta T \cong E_{kp}(1+R)k / (C_p\rho) = 56 \text{ K}.$$

Naturally, such a heating temperature cannot be the reason for LSEC ignition and a stimulus for phase transformations.

On the other hand, a heating temperature of optical absorbing microinhomogeneities (in our case, copper inclusions) can reach a much higher value. However, dependences of the ignition delay time on the energy density of laser radiation and sensitivity of EC on the binder concentration contradict the hypothesis of a 'purely thermal mechanism of the EC ignition', which occurs because of heating of optical microinhomogeneities.

The entire complex of experimental data indicates that LSEC ignition by short laser pulses depends largely on the material unloading by rarefaction waves. In our opinion, initiation is carried out according to the following mechanism. As a result of rapid heating of optical inhomogeneities ($\cong 10$ ns), due to thermoelastic stresses, shear deformations of a crystalline lattice occur in the microvolumes of the explosive adjacent to the inhomogeneities, being the cause of elementary chemical transformations; consequently, certain conditions arise for the formation of ignition centres. This statement is consistent with the results of quantum-mechanical calculations [50], in which, using the example of the simplest initiating explosive (silver azide), it was shown that crystalline structure decomposition (the interaction of N_3^- groups) can occur during shear deformation of the crystalline lattice (Fig. 6). Therefore, the substance unloading due to rarefaction waves, leads to the deformation relaxation of the material; consequently, it is the reason for 'quenching' of the reaction of blasting transformation of explosives. In the linear structure, $N \equiv \overset{e}{N} \equiv N$, the outermost N atoms are trivalent; their bound electrons are in the $1s^2 2s^2$ states; and the central atom is pentavalent, containing electrons in the $1s^2$ states. Thus, nitrogen atoms donate 5 electrons to the formation of a chemical bond, and the sixth electron is external, 'acquired' in the process of substance synthesis from the Ag atom. In general, AgN_3 is an ionic crystal [51].

When calculating the electronic therm of an ion N_3^-, it was assumed that valence electrons occupy the states of (1/2, 0, 0), (3/2, 0, 0), and (5/2, 0, 0). Angle α in the normal lattice state is 45°. The calculations assumed the change in angle α within the range of 45°–75°. This corresponds to shear deformations of the lattice within the range of angles 0°–30°. As we can see from the results shown in Fig. 6, an increase in lattice deformation results in a decreasing minimum energy therm

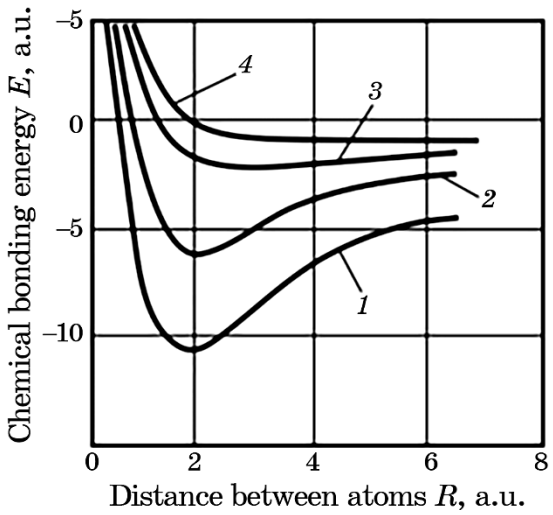

Fig. 6. Calculation of the AgN_3 structure stability during its deformation (angle α): 45° (*1*), 55° (*2*), 65° (*3*), 75° (*4*).

as well as in an increasing internuclear distance. Thus, deformation of the silver crystalline lattice is the cause of violation of group stability N_3^-, resulting in its decomposition (ionization) and, consequently, in the formation of chemically active radicals N_3, which interaction causes explosion blasting in terms of dense packing of atoms of a solid. Along with these calculations, the lattice stability was calculated under conditions of available interstitial defects by Ag ions in it. It is shown that in this case, when the lattice is deformed, its stability is reduced significantly.

3.3. Measurement of the LSEC Explosion Pulses

One of the most complicated problems in mechanics is study of the stability of structures that take the shock-wave loads. Rapid change in process parameters over time, available wave fronts, and formation of plastic zones in the material of construction—all the factors complicates significantly the study and makes us resort to a number of simplifying assumptions and hypotheses, being subject to experimental verification. In this regard, the role of experimental studies increases; they make it possible to obtain the necessary data on the material and structure behaviour under conditions of pulse action.

Particularly great difficulties arise in the studies dealing with the impact experienced by the structures from submicrosecond pulses of moderate intensity—0.1–1.0 kPa·s as there are no experimental methods for generating pulses of the specified range over large areas (more

than 1 m^2). For instance, such well-known shock-wave methods as hydraulic impact [27], air [52] and underwater explosion [53], and electric foil explosion [54] cannot implement fundamentally such an impact.

The interest in simultaneous initiation of the entire surface of an explosive layer coated over a large area is stipulated by the need for experimental modelling to simulate structural response of a material under the action of high-power pulsed x-ray radiation [55]. When the product surface is exposed to x-rays, the material evaporates as a result of rapid heating and generates a shock wave in the structure of the material, causing external and internal failures. While understanding the causes and mechanisms of destabilization of the system functioning to counteract them, various measures are taken at the design stage [56].

To implement a method of shock-wave treatment with a plane front of a detonation wave, a method of point initiation was excluded; a method was required for initiating a corresponding very sensitive explosive to a light pulse by a flash of light [57]. Paper [58] used a thin coating of silver–acetylene–nitrate silver explosive covering a relatively large area (up to 70 cm^2). The total duration of the light pulse exposure was about 6 μs. However, an impact with the duration of less than one microsecond can be satisfactory, which was not achieved by the authors of [59]. To simulate subshort pulses, it is necessary to search for new explosives being anomalously sensitive to the initiating action of a pulse light source. In this context, laser initiation of plane charges (diameter is 4.0 cm; thickness is 0.5 cm) made from a mixture of highly dispersed RDX and aluminium powders was studied in [60]. The energy density of laser radiation was 10 J/cm^2, more than two orders of magnitude higher than the values given in Table 2 for explosive composites [38]. To ignite by low-energy laser initiation, active research is being carried out to find safe primary explosives with low sensitivity to other initiating sources [61, 62].

To assess the possibility of achieving the required loading parameters, following conditions were accepted. A layer of explosives of thickness l is coated on the flat surface of the barrier under study. Depending on the type of explosive used, thickness of its layer, amount of the binder polymer, and wavelength of the initiating radiation, volumetric or surface ignition of the explosive is possible. In case of volumetric ignition, the explosive transformation covers simultaneously the entire explosive layer, since the pressure duration of the explosion products will depend on the propagation time of a rarefaction wave through the explosion products. The pressure on the barrier begins to drop when the wave is reflected from the barrier surface.

A satisfactory approximation for determining the transferred pulse magnitude can be the well-known solution of the problem of expansion of instantaneous detonation products [45]. A value of the pulse density is calculated by the formula

$$J_s = \xi\left(2m_s E_s\right)^{1/2}, \tag{25}$$

where m_s is mass of explosives per unit surface; E_s is internal energy of the detonation products; ξ is coefficient of proportionality, depending on the exponent of the adiabatic of the explosion products.

We can assume approximately that the value of E_s is proportional to the energy of chemical transformation at a constant volume Q. We consider that the adiabatic index of the explosion products is $\gamma = 3$. For this γ value, the proportionality coefficient is $\xi = 0.865$. Considering that $m_s = \rho l$, $E_s = Q\rho l$, we find from equation (25) that

$$l = J_s / \left(\xi Q \rho\right), \tag{26}$$

where ρ is density of the explosive.

Take lead azide as an example ($\rho = 4200$ kg/m^3, $Q = 1667$ kJ/kg) and determine the thickness of an explosive layer, which explosion generates a specific pulse of 0.1–1.0 kPa·s. It follows from (26) that $l \approx 0.02$–0.2 mm. The time of pressure action on the barrier can be estimated as follows:

$$t+ \geq 1 / C_H. \tag{27}$$

C_H is speed of sound in the explosion products. This estimate is valid since the barrier pressure after arrival of a rarefaction wave changes inversely proportionally to t^3 [45]

$$\left(P + / P_H\right) \geq \left(1 / C_H\right)^3. \tag{28}$$

Having substituted $C_H = 3700$ m/s, $l \approx 0.02$–0.2 mm in (28), we get $t \geq 10^{-8}$–10^{-7} s. Taking into account that the action of a detonation wave starts at the moment of its arrival to the wall and continues during the expansion time of the products in a rarefaction wave following a detonation wave, we can assume that the loading time will not exceed the values given above.

When the explosive surface is initiated, the plane front of a detonation wave propagates along the normal to the surface. The impact of the detonation product pressure begins at the moment a detonation wave arrives at the barrier surface ($t = l/D$, where D is detonation velocity of the explosive charge) and corresponds to the propagation time of a rarefaction wave through the explosion products.

The density of pulse transmitted to the barrier (rigid wall) is determined by the expression

$$J_s = 8\rho l D / 27. \tag{29}$$

Estimation of the explosive layer thickness according to expression

(29) ($D = 5500$ m/s for $\rho = 4200$ kg/m^3 [63]) results in $l \approx 0.015$–0.15 cm. Thus, to implement the pulse density 0.1–1.0 kPa·s, the coating thickness is obtained, if lead azide is used. Both considered schemes of explosive transformation of explosives give practically the same results. In real conditions, when using standard explosives, blasting devices, and initiation systems, it is fundamentally impossible to apply a layer of lead azide and initiate its entire surface. However, despite this, there is a way to achieve the required parameters of pressure pulses; it is based on laser initiation of detonation in coatings of light-sensitive explosive composites [64, 65]. Four LSECs that meet the requirements are represented in the following order: EC2—$4 \cdot 10^{-3}$ J/cm^2 (2.5 m^2), EC7—$5 \cdot 10^{-3}$ J/cm^2 (2.0 m^2), EC16—$8 \cdot 10^{-3}$ J/cm^2 (1.25 m^2), EC17—$40 \cdot 10^{-3}$ J/cm^2 (0.25 m^2).

The information in parentheses indicates the maximum possible areas of initiation by a laser pulse with the energy of 100 J. Figure 7 and Figure 8 show the dependences $J_s(m_s)$ for some LSECs. Experimental data were processed by the least squares method. As we can see from the figure, in terms of the same EC mass density, the maximum pulse of the explosion products is implemented upon laser initiation of VS17, which is smaller when VS2 is blasted; it is the lowest one when EC7 is blasted. On the other hand, extrapolation of the dependence $I_s(m_s)$ at $m_s \to 0$ (dashed lines) shows that $I_s(m_s)$ does not tend to zero, as it follows from the theory [49]. This means that a part of EC mass does not make a significant contribution to the recorded load pulse. Undoubtedly, this

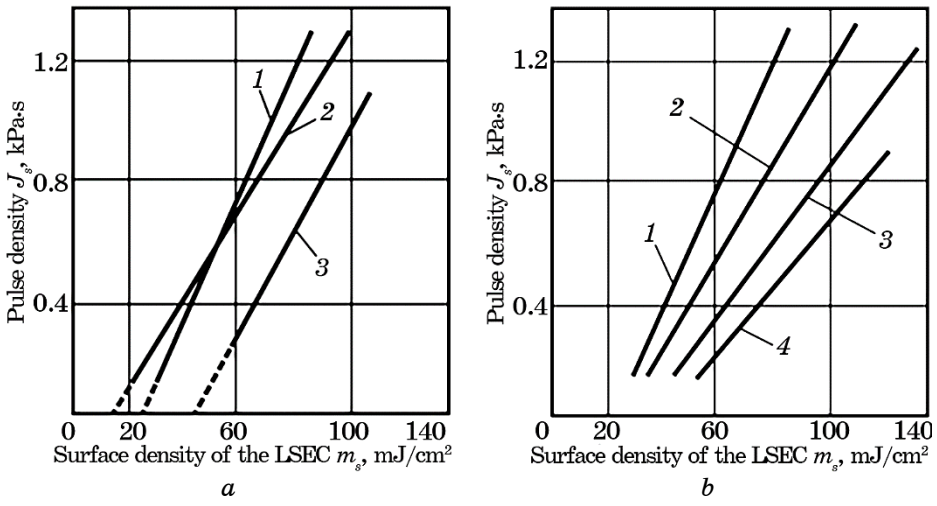

Fig. 7. Changes in the pressure pulse density depending on: LSEC grade [43] (*1*—EC2, *2*—EC17, *3*—EC7) (*a*); surface density of the mass at different concentration of binder material in composite EC2 (*1*—10%, *2*—20%, *3*—30%, *4*—40%) (*b*).

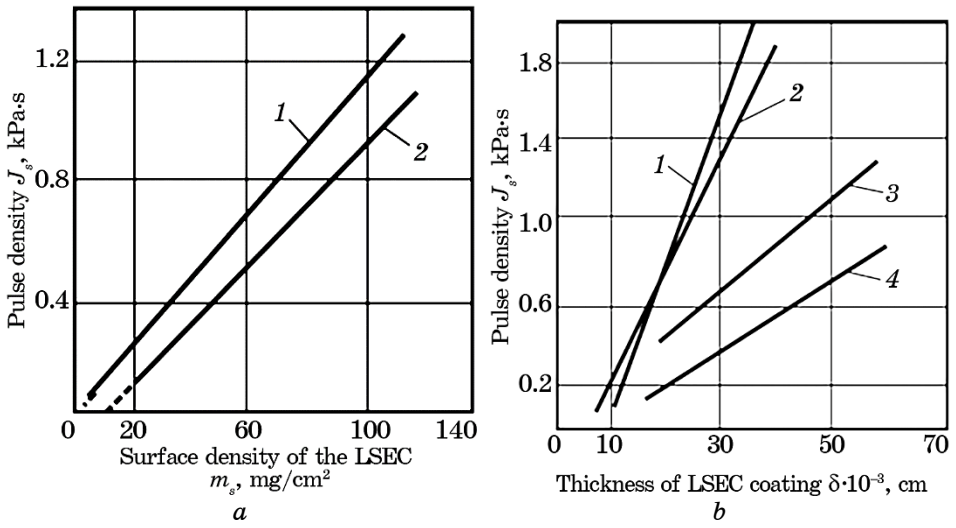

Fig. 8. Dependence of the pressure pulse density on the LSEC surface density: *a*—lead azide; *b*—lead azide + 20% of polymer (*a*); dependence of pulse density on the LSEC coating thickness: *1*—EC7; *2*—EC2; *3*—EC16, *4*—EC17 (*b*).

mass is consumed during the transition from combustion to detonation.

Figure 7 shows that along with the decreasing LSEC coating thickness, the pulse density goes down linearly. However, there are physicochemical limitations that do not allow obtaining arbitrarily small pulses. There is a certain coating thickness for each LSEC, at which detonation cannot be initiated even at such laser radiation energy densities that correspond to critical values of undermining massive (thick) samples at an increasing energy density of the initiating laser pulse. A further decrease in J_s is possible, but this reduces the possibilities of a loading method as a whole since the LSEC ignition area decreases. When undermining EC2 coating with a surface density of $m_s = 30$ mg/cm^2 (Fig. 7, *a*), the minimum value $J_s = 0.08$ kPa·s was obtained. During the experiments, J_s does not tend to zero at $m_s \to 0$, since it is due to the fact that the products of chemical reaction of some part of LSEC mass are consumed during the transition from combustion to detonation and do not contribute to the recorded pulse.

Figure 7, *b* demonstrates the results of measurements of pulse density as a function of the polymer mass concentration C_m for EC2 within the range from 10% to 40%. It can be seen that the increasing binder concentration results in the decreasing tangent of the slope of straight lines to m_s axis. This means that the EC detonation velocity decreases with the increasing polymer concentration. In addition, the material consumption for transition from combustion to detonation increases along with growing C_m. A pulse of a specified density can be imple-

mented using any of the represented explosive composites. For the same values of surface density m_s, the pulse durations of each of the composites will be different. To obtain the same pulse density, coatings of different thicknesses are required, *i.e.*, using composites of different formulations, it is possible to change the exposure duration in a certain range.

The pulse was determined using a pendulum [66, 67] on the samples with a surface mass density (10–100 mg/cm^2) of the composite. The voltage oscillograms show that the plane front of a shock wave degenerates into the spherical one [68]. This is indicated by the presence of a rarefaction region following the compression region. The compression pulse duration grows along with an increasing thickness of the composite coating. Within the specified range of the composite surface density (EC2, LSEC-1, EC17), the pulse duration did not exceed 0.7 μs.

A composite based on lead azide (LSEC-1), along with the composites of EC grade, can be used in studies of the resistance of structures to short (less than 1 μs) loads. However, only composite EC2 manages to receive loads within the range of pulse densities being 0.08–1 kPa·s.

Thus, the proposed method of loading, based on laser detonation of explosive compounds, makes it possible to obtain submicrosecond pulses with the intensity of 0.1–1.0 kPa·s. Taking into consideration the peculiarities of laser initiation, this method can be used when testing materials for strength.

The measurement error did not exceed 7%. The pendulum disks were made from those materials, for which it was necessary to obtain the characteristic dependences of the pulse density J_s on the LSEC surface density m_s. The dependences $J_s(m_s)$ represented below correspond to the loading of steel specimens. When measuring pulses, the same samples were used as in the study of sensitivity. The laser beam expanded, and the energy density at the centre of the beam exceeded by no more than 20% the energy density at the sample periphery. In addition, the average radiation energy density on the sample was twice the critical value. In this case, there was plane blasting of EC specimens, which was confirmed by the failure pattern of the materials loaded during the blasting of coatings made from EC grade composites with the area of 1 and 20 cm^2.

3.4. Plane and Linear Shock Waves

The method was tested by exposing a sample consisting of a three-layer material (Table 3) to a plane-wave front formed by a profiled detonation wave in the LSEC layer (Fig. 2). The first and second layers of the package were composite materials (CM). A polymer adhesive with a polymerization temperature of ≅ 250°C was used to connect firmly the layers. Experimental samples were made in the form of ∅ 50 mm circle.

TABLE 3. Characteristics of coatings.

Coating material	Material composition	Thickness, mm	Speed of sound, m/s
MFP-1	Carbolon	3	1250
	TTP-KS	3	800
	AMG-6	2.5	1900
MFP-2	UP-E	3	950
	TTP-KS	3	80
	AMG-6	2.5	1900

A LSEC coating of EC2 with a thickness of 1.2–1.5 mm was applied to the CM surface. The laser beam diameter was 70 mm; the average energy density in the beam was 1.5–2 times higher than the EC2 sensitivity. The features of impact of various-profile shock waves on the material were studied by a comparative analysis of the pattern of three-layer material failure (Fig. 7).

When a plane detonation wave front was formed by the action of a laser pulse on LSEC or a plane shock wave in a target consisting of several layers of different materials, simple estimate was made concerning the minimum loading area size. It was assumed that the maximum tensile stresses in the material arise at the moment of the reverse rarefaction wave arrival on the sample surface. This time can be estimated from the formula

$$t_p = \left(r / D_{sh}\right) + \left(r / C_{\min}\right),$$

where r is sample thickness, D_{sh} is shock wave velocity, $C_{\min}$ is minimum value of the speed of sound of the materials included in the sample. Obviously, such an estimate gives an overestimated value of t_p.

The maximum distance, to which a lateral rarefaction wave will propagate during this time, will not exceed the value of $d = C_{\max} t_p$, where $C_{\max}$ is maximum value of the speed of sound.

Thus, to ensure the impact of the shock wave plane front on MFP, it is necessary that the size of area loaded by a plane wave exceeds the d value. Basing on this condition, it follows that the plane loading condition is ensured on a site, which diameter is not less than

$$d = 2C_{\max}\left\{\left(r / D_{sh}\right) + \left(r / C_{\min}\right)\right\} = 50 \text{ mm}.$$

Here, the shock wave velocity was taken equal to the detonation velocity of the light-sensitive explosive composite used in the experiment ($D_{sh} = 6500$ m/s).

To obtain a plane shock wave front, the sample was mounted in such

a way that, under the action of a light pulse, detonation was excited simultaneously on the entire LSEC irradiated surface (Fig. 2). In this way, a plane detonation wave was formed, propagating along the normal to the surface of a three-layer coating sample (MFP). Interaction of a direct rarefaction wave following a shock wave and a backward wave that occurs, when a shock wave reaches the rear surface of the sample led to delamination of the central part of the three-layer package along the boundary of the first (I) and second (II) composite material. At the periphery of the sample, delamination was observed along the boundary of the second and aluminium layers (III); it is explained by the influence of a lateral unloading wave on the material deformation process. Thus, as a result of the plane-wave action of a shock wave, the aluminium plate delaminates (Fig. 9, *a*).

To obtain sliding detonation waves, a part of the surface of film charges was covered with a screen. In this context, an annular detonation wave, converging to the sample centre, impacted as follows. The central sample part was covered with an opaque screen (black paper) in the form of a circle; its diameter was 2 mm smaller than the diameter of LSEC coating and, accordingly, the sample. Thus, the LSEC initiation occurred along a ring of 1 mm thick. The failure pattern differs from the one of the entire sample surface by a plane wave front. Along with the package delamination along the boundary (I)–(II), one can observe a rupture of the upper material along a circle with the diameter

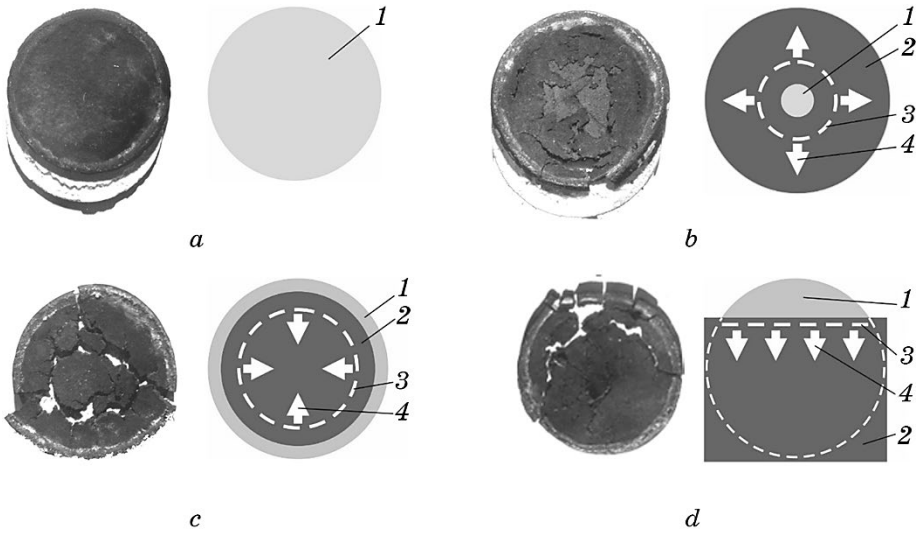

Fig. 9. Failure pattern of a three-layer material sample influenced by a shock wave: plane wave (*a*), wave converging to the centre (*b*), wave diverging from the centre (*c*), linear wave (*d*), open LSEC surface (*1*), screen (*2*), detonation front (dashed line) (*3*), direction of the front movement (arrows) (*4*).

of ≅ 40 mm. This discontinuity is stipulated by the action of a lateral rarefaction wave following the material behind an oblique shock wave moving towards the sample centre. The failure pattern is shown in (Fig. 9, *b*).

A detonation wave front diverging from the sample centre to its periphery (an annular wave front) was formed by laser initiation of the LSEC layer in the sample centre, which was covered preliminarily with paper with a central hole of 4 mm in diameter. Interaction of a rarefaction wave following an oblique shock wave and a rarefaction wave generated by the reflection of an oblique shock wave from the rear side of the packet leads to the sample delamination along the boundary (I)–(II). The output of a shock wave on the lateral surface of the three-layer package generates an unloading wave, which interaction with a rarefaction wave results in breaking of the outer material of the package. Typical failure pattern is shown in Fig. 9, *c*.

A sliding linear detonation wave was obtained by laser illumination of an open segment being 12.5 mm high (Fig. 9, *d*). Obviously, the failure pattern is determined by the profile of a sliding detonation wave. As we can see in Fig. 9, the failure pattern depends on the initiation conditions. The results of the experiments indicate that use of screens makes it possible to form a sliding detonation wave front from a linear shape to any configuration that is necessary to solve the problems of shock wave processing of materials.

The methodology for studying the effect of a plane detonation front on the stability of materials (especially the multilayer ones) was complemented by certain changes in the values of pulses affecting the materials. The pulses were changed by altering the mass of a photosensitive explosive composite.

An analysis of the obtained experimental results showed that the pattern of shock-wave failure of the outer layer of the MFP sample depends on the pulse magnitude of the acting shock wave [69, 70]. Thus, failure of carbolone (MFP-1) is observed when loading with a pulse of 1.42 kPa·s, and failure of UP-E is observed at 0.58 and 1.42 kPa·s. Regardless of the pulse magnitude, a plate from AMG-6 is detached from the middle layer of the MFP—TTP-KS. When loaded with pulses of 0.3 and 0.58 kPa·s, detachment occurs at the place of gluing; at 1.42 kPa·s, the AMG-6 plate detaches from MFP as a result of failure of the middle layer—TTP-KS.

Different pattern of the plate detachment from AMG-6 is explained by different magnitude of a load pulse. At low pulse values, as a result of interacting incident and reflected rarefaction waves, the maximum tensile stresses arise in a plane located near the rear side of MFP, leading to AMG plate delamination from TTP-CS within the gluing area. At high values of pulses, the plane of maximum tensile stresses is closer to the middle layer of CM, resulting in its failure.

Failure pattern of the second layer of the substance indicates that laser initiation of a large-area of LSEC surface results actually in plane-wave loading of materials. Rupture of the second layer of MFP material at maximum loads as well as its plane geometry indicates that plane rarefaction waves—incident and reflected ones—play a decisive role in the destruction process. The results of the experiments specify the decisive role of the interaction of rarefaction waves in the process of material failure under mechanical pulse loads [71]. The main idea of these experiments was to change the place where rarefaction waves meet by using a liquid as a damper, which linear size towards normal to the sample surface exceeded significantly the sample thickness. The wave impedance of the damper had to correspond to the wave impedance of AMG-6 to exclude the formation of a reflected shock wave.

While performing studies with laser initiation by light-sensitive composites, it should be noted that an increase in the binder material concentration is accompanied by growing transparency of the LSEC samples along with the increasing area of radiation exposure to the material, being similar to an increase in the sample thicknesses. The process of laser ignition is determined largely by radiation scattering in the LSEC samples. A dependence of LSEC sensitivity on the thickness was identified, indicating a significant role of an unloading wave in the initiation and development of a chemical reaction in the bulk explosive composite.

3.5. Converging Cylindrical Shock Waves

Scientific interest in converging cylindrical detonation and shock waves was initiated by the results of studies published within the period of 1940s–1950s. Thus, for the first time, G. Guderley proposed a physical and mathematical model of a converging cylindrical front of a shock wave [72]. L. D. Landau and K. P. Staniukovich established an asymptotic law of pressure growth as the axis of a cylindrical detonation wave front is approached; the law is described in Ref. [45]. Ya. B. Zeldovich proposed a scenario for the onset of the convergence process and a mechanism for amplification of the cylindrical detonation wave front [73].

The relevance of studies concerning the problem of stability of converging cylindrical and spherical shock and detonation waves is evidenced by the results of studies analysing stability of cylindrical converging detonation waves in a gaseous explosive [74], in air [75] as well as studies of the patterns of motion and causes of instability, which affects principally the energy concentration behind the front of a converging shock wave [76] with the allowance for nonlinear heat conduction [77]. In this context, studies of cumulation, pulse, and energy in converging shock waves were especially actively developed; attention

was paid to flows in the vicinity of the transition point of an overcompressed cylindrical and spherical detonation wave to the Chapman–Jouguet regime [78–80].

A converging cylindrical detonation wave is formed according to the principle of the formation of a plane-wave front in the LSEC charge. The experiment was distinguished by the fact that the outer lateral surface of a cylindrical steel pipe with the applied LSEC layer was covered with laser radiation (Fig. 10). If a similar scheme of the experiment described in [71] provides for adjustment of the laser beam path using 12 interdependent elements (mirrors, diaphragms, diverging lenses, dividing plates), the device in Fig. 10 has only two elements of that kind: a diaphragm and a lens; however, four (or three) lasers are used.

The studies dealing with the formation of a converging front of a cylindrical shock wave [81] used the idea of initiating detonation of the entire LSEC surface exposed to laser radiation [64]. The following positive results were obtained in studies [81]. The excitation of detonation occurred simultaneously on the lateral surface of a cylindrical container. Evidence of strictly symmetrical compression is the position of the container after the explosion—at the site of its installation before explosion. The shocked material was preserved, and the container was not damaged. The calculated values of the shock wave parameters were achieved; they corresponded to the p, T-conditions for the transition of

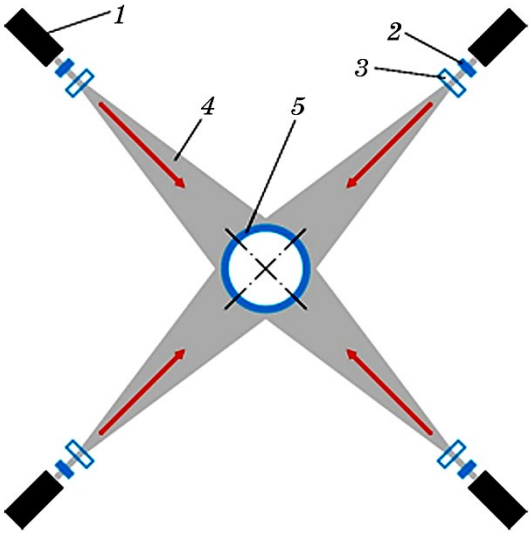

Fig. 10. Scheme of a device for forming a converging front of a cylindrical detonation (shock) wave: laser (*1*), diaphragm (installation level—0.3) (*2*), diverging lens (*3*), expanded laser beam (*4*), LSEC layer covering a lateral surface of a cylindrical pipe (diameter is 30 cm; wall thickness is 0.7 cm; height is 30 cm) (*5*).

graphite into diamond. One laser and 13 interdependent elements (*5* mirrors, *1* diaphragm, *4* lenses, *3* dividing plates, and *1* diaphragm) were used in the cylindrical wave formation scheme, which complicated significantly the adjustment of the laser path.

A device diagram shown in Fig. 10 distinguishes with a simpler setup of the laser path, which runs separately from each of the four lasers. The beams of four lasers included in a single electronic network with almost identical energy characteristics (Table 1) irradiate synchronously the lateral surface of a cylindrical pipe, on which the LSEC layer, being 1.7–2.2 mm thick, is applied. If EC17 is used, the exposure time is 0.25–0.3 μs. As a result of laser pulse radiation, the LSEC lateral surface detonates simultaneously. After the LSEC explosion, the cylindrical pipe remained at the place of its installation, which indicates a uniform shock-wave compression of the lateral surface of the pipe. Maximum duration of impact pressure is about 0.1 μs.

Since the energy distribution in the beam is consistent with the Gaussian distribution (Fig. 5), when the beam is expanded by a lens, the distribution will also be Gaussian but extended along with the increasing area. The energy density distribution in a Gaussian beam with radial symmetry can be specified as [82]:

$$E(r) = \frac{W}{2\pi\sigma^2}\exp\left(-\frac{r^2}{2\sigma^2}\right). \tag{30}$$

Function (30) is normalized to the total laser pulse energy $W 2\pi\int_0^\infty E(r)\,rdr = W$. Parameter σ determines the Gaussian curve shape; there is a specific value for each laser installation.

As a rule, the experiments on LSEC laser initiation involve Gaussian beams limited by a diaphragm in terms of the radiation intensity level *p*. The diaphragm radius is determined from the condition:

$$p = \frac{E(r)}{E(0)} = \exp\left(-\frac{r_0^2}{2\sigma^2}\right), \tag{31}$$

where $E(0) = W/(2\pi\sigma^2)$ is energy density at the beam centre.

Since the unexpanded beam passes through the diaphragm, the beam radius, at the intensity level *p*, is determined by the expression

$$r_0 = \sqrt{2\sigma^2 \ln(1-p)}. \tag{32}$$

From (32), express the Gaussian parameter σ in terms of radius r_p of the expanded beam at level *p* in some section of the beam

$$\sigma = r\left[2\ln(p-1)\right]^{-0.5}.$$

The expanded beam radius at distance R from the focus of the lens is expressed as follows

$$r_p = \frac{d}{2F} R, \tag{33}$$

where d is diaphragm diameter, F is focal length of the lens, R is distance from the lens focus to the pipe axis.

We select r_p so that the expanded beam illuminates the entire surface of a cylinder, visible from the laser installation site. In addition, its beam radius must be more than half the diagonal of the axial section of the cylindrical pipe (according to the practice, by 10–15%):

$$r_p > \frac{1}{2}\sqrt{H^2 + (2r)^2}, \tag{34}$$

where H is height of the pipe, r is radius of the cylinder.

The distribution function of the laser energy density was calculated using the initial geometric characteristics of the pipe, the distance from the lens focus to the pipe axis being 1000 cm, the height being $z = H/2$, and the energy characteristics of laser radiation.

The minimum value of the distribution function E is $2.162 \cdot 10^{-4}$ cm^{-2}, the maximum one is $2.516\ 10^{-4}$ cm^{-2}.

Let us estimate the energy value of the laser pulse. Energy density distribution is

$$E(\theta, z) = EW, \tag{35}$$

where W is total energy per pulse.

We select a value of the critical energy density for LSEC; moreover, we select the maximum of the given values in Table 2:

$$E(\theta, z) = 40 \text{ mJ / cm}^2.$$

Energy W falls on each of the four sides; we will find the energy from (35)

$$W = 4E(\theta, z) / E.$$

While substituting the numerical values, we determine $W = 40 \text{ mJ/cm}^2 / 2.162 \cdot 10^{-4} \text{ cm}^{-2} \approx 183 \text{ J}$. Such a pulse energy value is quite achievable by stationary laser installations, which can be used during industrial application of the laser initiation method for dynamic pressure processing.

Explosive composites, being photosensitive to a laser pulse, and new means of blasting and detonation initiation developed on their basis

make it possible to perform shock-wave processing of materials in terms of cylindrical cumulation of shock waves and, at the same time, preserve reliably the material after its shock compression.

4. CONCLUSIONS

Formation of detonation and shock waves of a specified profile makes it possible to increase significantly the dimensions and, accordingly, the workpiece surface, reduce the mass of explosives consumed, automate the process of explosion preparation and conduct, increase a degree of personnel safety, improve significantly the accuracy of blasting, and enhance environmentally positive effect when using 'green' light-sensitive composites. A laser method of detonation excitation helps standardize future physical experiments on the material processing by shock waves.

The effect of laser initiation of a converging cylindrical front of a detonation wave in a thin layer of a cylindrical LSEC charge is advisable to use for developing a methodology to test strength of materials of various airframes, stability of cylindrical shells (structures). The use of unique explosive characteristics of light-sensitive explosive composites and a laser method of detonation excitation of the whole surface coated with the composite can simulate quite satisfactorily the pulse effects (less than 1 μs) of x-ray and ultraviolet radiation from the combat laser systems on the area (up to 4 m^2). This technique is the only one that allows loading simultaneously the structure surface and implementing the required parameters of pulse loading. The research was tested during strength tests of multifunctional coatings of missile bodies.

Studies of the ignition process of light-sensitive explosive composites with wide laser beams have made it possible to develop a method for influencing materials with profiled shock waves for throwing plates and shells, and strengthening the complex-surface materials. Metal shells were tested for strength under the action of pulse mechanical loads of microsecond duration and moderate intensity of 0.1–1.0 kPa·s.

The uniqueness of the technique for initiating detonation in explosive charges with a specified wave front profile makes it possible to simulate fully the real action of an x-ray laser on a test sample, being one of the important means of modelling the structural response of high-power pulsed x-ray radiation; in addition, it is possible while using an experimental laser with the power of about 1000 less than the combat one. That also helps widen a range of products in the field of metal hardening by explosion, especially in terms of large-sized products.

The authors express their gratitude to General Director of the State Enterprise "Scientific and Production Association 'Pavlohrad Chemical Plant'", Corresponding Member of the N.A.S. of Ukraine, Dr.

Tech. Sciences Leonid Shyman, Director of the Research Institute of High-Energy Materials, Dr. Tech. Sciences, Prof. Yevhenii Ustymenko, and Technologist, Ph.D. in Tech. Sciences Oleksii Kyrychenko for the assistance in organizing and conducting the experimental studies.

REFERENCES

1. V. V. Danilenko, *Solid State Phys.*, **46**, No. 4: 581 (2004) (in Russian).
2. E. A. Petrov, *Detonation Synthesis of Nanomaterials. Nanodiamonds and Nanotechnologies* (Biysk: Altai STU: 2015) (in Russian).
3. N. Roy. Greiner, D. S. Phillips, J. D. Johnson, and F. Volk, *Nature*, No. 333: 440 (1988).
4. P. S. De Carly and I. L. Jamieson, *Science*, **133**, Iss. 3467: 1821 (1961).
5. G. A. Adadurov, A. V. Baluev, O. N. Breusov, V. N. Drobyshev, A. I. Rogacheva, A. M. Sapegin, and V. F. Tatsiy, *Bulletin of AS USSR. Inorganic Materials*, **4**: 649 (1977) (in Russian).
6. V. V. Sobolev, S. I. Gubenko, D. V. Rudakov., O. L. Kyrychenko, and O. O. Balakin, *Naukovyi Visnyk Natsionalnoho Hirnychoho Universytetu*, **4**: 53 (2020).
7. V. V. Sobolev, R. P. Didik, V. Ya. Slobodskoi, Y. I.Merezko, and A. I. Skidanenko, *Combustion, Explosion, and Shock Waves*, **19**, No. 5: 658 (1983).
8. V. V. Sobolev, O. S. Kovrov, M. M. Nalisko, N. V. Bilan, and O. A. Tereshkova, *Naukovyi Visnyk Natsionalnoho Hirnychoho Universytetu*, **4**: 47 (2021).
9. A. V. Kurdyumov and A. N. Pilyankevich, *Phase Transformations in Carbon and Boron Nitride* (Kiev: Naukova Dumka: 1979) (in Russian).
10. V. V. Yakushev, A. N. Zhukov, A. V. Utkin, A. I. Rogacheva, and V. A. Kudakina, *Combustion and Eexplosion Physics*, **51**, No. 5: 104 (2015).
11. A. N. Zhukov, S. E. Zakiev, and V. V. Yakushev, *High Temperature Thermophysics*, **54**, No. 1: 51 (2016) (in Russian).
12. V. V. Sobolev, R. P. Didyk, V. Ya. Slobodskoy, V. P. Baraban, S. N. Selyukov, A. I. Skidanenko, and A. A. Udoev, *Mineralogical Collection of Lvov University*, **39**, No. 2: 75 (1985) (in Russian).
13. Z. Wang, Y. Zhao, K. Tait, X. Liao, D. Schiferl, C. Zha, T. Downs, J. Qian, Y. Zhu, and T. Shen, *Proc. Natl. Acad. Sci. U. S. A.*, **101**, No. 38: 13699 (2004).
14. V. V. Sobolev, V. Ya. Slobodskoi, S. N. Selyukov, and A. A. Udoev, *Int. Geol. Rev.*, **28**, No. 6: 680 (1986).
15. R. V. Eliseev, *Bulletin of the KrNU named after Mikhail Ostrogradsky*, **2**, Iss. 73: 74 (2021) (in Ukraine).
16. A. A. Deribas, *Physics of Hardening and Explosive Welding* (Novosibirsk: Nauka: 1980) (in Russian).
17. A. V. Krupin, V. Ya. Soloviev, N. I. Sheftel, and A. G. Kobelev, *Deformation of Metals by Explosions* (Moskva: Metallurgiya, 1975) (in Russian).
18. E. A. Kozlov, M. A. Lebedev, and B. V. Litvinov, *Combustion and Explosion-Physics*, **2**: 118 (1993) (in Russian).
19. L. V. Altshuler, *Advances of Physical Sciences*, **65**, No. 5: 197 (1965) (in Russian).
20. R. F. Trunin, *Properties of Condensed Substances at High Pressures and Tem-*

peratures (Sarov: RFNC FNIIEF: 1992) (in Russian).
21. M. V. Zhernokletov, *Methods for Studying the Properties of Materials under Intense Dynamic Loads* (Sarov: RFNC VNIIEF: 2005) (in Russian).
22. V. V. Danilenko, *Explosion: Physics, Techniques, Technology* (Moscow: Ehnergoatomizdat: 2010) (in Russian).
23. G. I. Kanel, V. E. Fortov, and S. V. Razorenov, *Advances of Physical Sciences*, **177**, No. 8: 809 (2007) (in Russian).
24. P. Caldirola and H. Knoepfel, *Physics of High Energy Densities* (Moskva: Mir: 1974) (Russian translation).
25. S. G. Andreev, M. M. Boyko, and V. V. Selivanov, *Experimental Methods of Explosion and Impact Physics* (Moskva: Fizmatlit: 2013) (in Russian).
26. G. Ben-Dor, O. Igra and T. Elperin, *Handbook of Shock Waves. Vol. 2* (San Diego: Academic Press: 2001).
27. V. E. Mineev, *Research on the Theory of Plates and Shells. Kazan: KGU*, Nos. 6–7: 596 (1970) (in Russian).
28. A. V. Karmishin, E. D. Skurlatov, and V. G. Startsev, *Nonstationary Aeroelasticity of Thin-Walled Structures* (Moskva: Mashinostroyenie: 1982) (in Russian).
29. A. V. Chernai, V. V. Sobolev, V. A. Chernai, M. A. Ilyushin, and A. Dlugashek, *Combustion and Explosion Physics*, **39**, No. 3: 105 (2003).
30. V. V. Sobolev, A. V. Chernai, and M. A. Ilyushin, *Chemical Physics of Combustion and Explosion Processes*, **1**, No. 1: 80 (Chernogolovka: CHIF RAN: 1996) (in Russian).
31. A. V. Chernai, V. V. Sobolev, M. A. Ilyushin, V. A. Chernai, and A. D. Sharabura, *High Pressure Physics and Technology*, **11**, No. 3: 94 (2001) (in Russian).
32. M. A. Ilyushin, I. V. Tselinskii, and A. M. Sudarikov, *Development of Components for High-Energy Compositions* (St. Petersburg: Leningrad State University named after A. S. Pushkin: 2006) (in Russian).
33. V. V. Sobolev, A. V. Chernai, and N. M. Studinskii, *High-Energy Processing of Materials*, **1**: 136 (Dnepropetrovsk: SMAU: 1995) (in Russian).
34. M. A. Ilyushin, I. V. Tselinsky, and I. V. Shugalei, *Cent. Eur. J. Energ. Mater.*, **9**, No. 4: 293 (2012).
35. M. A. Ilyushin, I. V. Tselinskii, I. A. Ugryumov, A. Yu. Zhilin, and A. V. Chernai, *Collection of Scientific Papers. NMAU*, **18**: 8 (2003) (in Russian).
36. M. A. Ilyushin, I. V. Tselinskii, I. V. Shugalei, and A. V. Chernai, *Pulse Processing of Materials* (Dnepropetrovsk: NMU: 2005) (in Russian).
37. M. A. Ilyushin, I. V. Tselinskii, A. A. Kotomin, and Yu. A. Danilov, *Energy Saturated Substances of Initiation Means* (St. Petersburg: Leningrad State University named after A. S. Pushkin: 2013) (in Russian).
38. M. A. Ilyushin, A. V. Smirnov, and A. M. Sudarikov, *Metal Complexes in High-Energy Compositions* (St. Petersburg: Leningrad State University named after A. S. Pushkin: 2010) (in Russian).
39. A. V. Chernai, V. V. Sobolev, V. A. Chernaj, M. A. Ilyushin, and A. Dlugashek, *Combustion, Explosion and Shock Waves*, **39**, No. 3: 335 (2003).
40. A. L. Kirichenko, V. V. Kulivar, and V. V. Sobolev, *Bulletin of Donetsk Mining Institute*, **2**: 141(2017) (in Russian).
41. V. V. Sobolev and V. V. Kulivar, *III International Scientific and Practical Con-*

ference 'Society and Science. Problems and Prospects' (January 25–28, 2022, London, England).
42. V. V. Sobolev, L. N. Shiman, N. N. Nalisko, and A. L. Kirichenko, *Naukovyi Visnyk Natsionalnoho Hirnychoho Universytetu*, **6**: 53 (2017) (in Russian).
43. A. V. Chernaj, V. V. Sobolev, M. A. Ilyushin, N. E. Zhitnik, *Fizika Goreniya i Vzryva*, **30**, No. 2: 106 (1994) (in Russian).
44. A. V. Chernai, V. V. Sobolev, V. A. Chernai, A. Dlugasek, D. Berezovsky, and M. A. Ilyushin, *Collection of Scientific Papers. NMAU, High-Energy Processing of Materials*, **8**: 214 (Dnepropetrovsk: Sich: 1999) (in Russian).
45. K. P. Stanyukovich, *Unsteady Motions of a Continuous Medium* (Moskva: Nauka: 1971) (in Russian).
46. Ya. B. Zeldovich and Yu. P. Raiser, *Physics of Shock Waves and High-Temperature Hydrodynamic Phenomena* (Moskva: Nauka: 1966) (in Russian).
47. A. N. Afanasenkov, *Blasting Work*, *75/32* (Moskva: Nedra: 1975) (in Russian).
48. A. N. Dryomin, S. D. Savrov, V. S. Trofimov, and K. K. Shvedov, *Detonation Waves in Condensed Media* (Moskva: Nauka: 1970) (in Russian).
49. F. A. Baum, A. P. Orlenko, K. P. Stanyukovich, V. P. Chelyshev, and B. I. Shekhter, *Physics of Explosion* (Moskva: Nauka: 1975) (in Russian).
50. A. V. Chernai, V. V. Sobolev, V. A. Chernai, M. A. Ilyushin, and Yu. P. Bunchuk, *Physics of Pulse Processing of Materials* (Dnipropetrovsk: ART-PRESS: 2003) (in Russian).
51. F. Bowden and A. Ioffe, *Fast Reactions in Solids* (Moskva: Foreign Literature: 1962) (in Russian).
52. L. T. Sedov, *Similarity and Dimension Methods in Mechanics* (Moskva: Nauka: 1987) (in Russian).
53. R. Cole, *Underwater Explosions* (Moskva: Foreign Literature: 1950) (in Russian).
54. D. Keller and J. Penning, *Synthesis Microstructure and Explosive Properties of Spray-Deposited Silver Acetylide-Silver Nitrate Composite Light Initiated High Explosives* (Albuquerque, NM, USA: Sandia National Laboratories: 1965).
55. D. V. Keller and J. R. Penning, *Exploding Wires*, **2**: 263 (1962).
56. T. T. Covert and M. A. Chavez, *Synthesis Microstructure and Explosive Properties of Spray-Deposited Silver Acetylide-Silver Nitrate Composite Light Initiated High Explosives* (Albuquerque, NM, USA: Sandia National Laboratories: 2013).
57. S. Silverman, *Tech. Report*, No. 1, Project No. 02-1770 (IR) (San Antonio, Texas: Southwest Research Institute: December 1965).
58. F. O. Hoese, C. G. Angner, and W. E. Baker, *Exp. Mech.*, **8**: 392 (1968).
59. D. Wang, J. Li, Yu. Zhang, H. Li, and S. Wang, *Materials*, 15, No. 12: 4100 (2022).
60. N. P. Khokhlov, N. A. Ponkin, I. A. Lukyanenko, A. V. Rudnev, O. M. Lukovkin, Y. V. Sheikov, and S. M. Batyanov, *Combust. Explos. Shock Waves*, **57**, No. 3: 364 (2021).
61. T. W. Myers, K. E. Brown, D. E. Chavez, R. J. Schaarff, and J. M. Veauthier, *Inorg. Chem.*, **56**, No. 4: 2297 (2017).
62. V. Y. Wurzenberger, M. S. Gruhne, M. Lommel, and J. Stierstorfer, *Propellants Explos. Pyrotech.*, **46**: 207 (2021).
63. A. F. Chumak, A. D. Vlasov, and L. I. Muravina, *Combustion and Explosion Physics*, **13**, No. 4: 650 (1977).

64. A. V. Chernai and V. V. Sobolev, *Fizika i Khimiya Obrabotki Materialov*, No. 5: 120 (1995) (in Russian).
65. A. V. Chernai, V. V. Sobolev, N. M. Studinskii, and I. L. Gumenik, *Metallurgical and Mining Idustry*, No. 1: 47 (1995) (in Russian).
66. A. Chernai, V. Sobolev, and N. Nalisko, *J. Scientific Israel-Technological Advantages*, **18**, No. 3: 98 (2016).
67. M. Nalisko, V. Sobolev, D. Rudakov, and N. Bilan, *E3S Web of Conferences 123*, 01008 (Ukrainian School of Mining Engineering: 2019).
68. L. D. Landau and E. M. Lifshitz, *Continuum Mechan*ics (Moskva: Gostekhizdat: 1954) (in Russian).
69. A. V. Chernai, V. V. Sobolev, M. A. Ilyushin, and N. E. Zhitnik, *Combustion, Explosion, and Shock Waves*, **30**, No. 2: 239 (1994).
70. A. V. Chernai, V. V. Sobolev, V. A. Chernai, M. I. Ilyushin, and A. Dlugashek, *Collection of Scientific Papers. NMAU High-Energy Processing of Materials*, No. 8: 221 (Dnepropetrovsk: Sich: 1999) (in Russian).
71. A. V. Chernai, V. V. Sobolev, M. I. Ilyushin, and V. A. Mazarchenkov, *Industrial Explosives and Means of their Initiation (Shostka, Sumy Region: GosNIIKhP)*, Iss. 1: 56 (1995) (in Russian).
72. G. Guderley, *Zylinderachse, Luftfahrtforschung*, **19**, No. 9: 302 (1942).
73. Ya. B. Zeldovich, *J. Exp. Theor. Phys.*, **36**, No. 3: 783 (1959) (in Russian).
74. R. Knystautas and J. H. Lee, *Combust. Flame*, **1**, No. 1: 61 (1971).
75. K. Takayama, H. Kleine, and H. Grönig, *Exp. Fluids*, **5**: 315 (1987).
76. A. N. Golubyatnikov, S. I. Zonenko, and G. G. Cherny, *Applied Mathematics and Mechanics*, **71**, No. 5: 727 (2007).
77. A. A. Makhmudov and S. P. Popov, *Fluid and Gas Mechanics*, **2**: 167 (1980) (in Russian).
78. E. I. Zababakhin and V. A. Simonenko, *Applied Mathematics and Mechanics*, **29**, No. 2: 334 (1965) (in Russian).
79. A. N. Golubyatnikov, S. I. Zonenko, and G. G. Cherny, *Adv. Mech.*, **3**, No. 1: 31 (2005) (in Russian).
80. S. I. Zonenko and G. G. Cherny, *Reports of the Academy of Sciences*, **390**, No. 1: 46 (2003) (in Russian).
81. V. V. Sobolev, O. V. Skobenko, I. I. Usyk, V. V. Kulivar, and A. V. Kurliak, *Naukovyi Visnyk Natsionalnoho Hirnychoho Universytetu*, **6**: 49 (2021).
82. V. V. Sobolev, D. V. Rudakov, A. S. Baskevich, and A. L. Kirichenko, *Physical and Mathematical Models in Problems of Laser Lnitiation of Explosives* (Kyiv: SP Burya E. D.: 2020) (in Russian).